

# The Thermal Properties of Poly(pivalolactone)

Janusz Grebowicz

Shell Development Company, Westhollow Research Center, P.O. Box 1380, Houston, TX 77701, U.S.A.

Manika Varma-Nair and Bernhard Wunderlich

Department of Chemistry, University of Tennessee, Knoxville, Tennessee 37996-1600 and Chemistry Division of Oak Ridge National Laboratory, Oak Ridge, Tennessee 37831-6197, U.S.A.

## ABSTRACT

Quantitative thermal analysis was carried out for poly(pivalolactone) (PPVL), including heat capacity determinations from 140 to 550 K. The experimental  $C_p$  below the glass transition temperature was fitted to an approximate vibrational spectrum and the ATHAS computation scheme was used to compute the "vibration only" heat capacities from 0.1 to 1000 K. The liquid  $C_p$  was derived from an empirical addition scheme and found to agree with the experimental  $C_p$  with an RMS of  $\pm 2.8\%$  from 240 K to 550 K. A glass transition,  $T_g$ , could be detected at 260 K, and the change in heat capacity for 100% amorphous PPVL was calculated to be 38.8 J/(K mol). Above  $T_g$ , semicrystalline samples seem to show a rigid amorphous fraction that does not contribute to the increase in heat capacity at  $T_g$ . Using the ATHAS recommended heat capacities, the various thermodynamic functions (enthalpy, entropy, and Gibbs function) were derived. The residual entropy at 0 K for the amorphous PPVL was calculated to be 5.2 J/(K mol) per mobile bead, and was comparable to that obtained for a series of linear, aliphatic polyesters analyzed earlier.

**KEYWORDS:** Thermal analysis, Heat capacity, Rigid amorphous, Glass transition, Poly(pivalolactone)

## INTRODUCTION

Poly(pivalolactone), or poly( $\alpha,\alpha'$ -dimethylpropiolactone) (PPVL), has been shown earlier to exhibit polymorphism. It exists in two crystal forms,  $\gamma$  (which consists of chains with a 4 $\times$ 3/1 helix) and  $\alpha$  (which has a 4 $\times$ 2/1 helix) [1]. The  $\gamma$  samples consist of

low melting crystals (about 448 K) [2]. They are formed on fast cooling from the melt. With increasing crystallization time at a given temperature, the  $\gamma$  crystals convert to the high melting  $\alpha$  form. Borri *et al.* [2] have investigated the crystallization behavior in considerable detail. Isothermal crystallization at increasing temperatures (403–493 K) decreases the amount of low melting material and increases its melting peak temperature from about 448 K until it merges with the high-temperature melting peak at about 473 K. The high-temperature melting peak does not change with the crystallization temperature. PPVL represents, thus, an example where the low-temperature crystals are not only of less perfection, but also consists of a metastable crystal form [3]. A third crystal form ( $\beta$ ) has been observed on deformation of the sample [1]. The equilibrium melting temperature, as estimated from highest observed melting, was reported to be at 513 K and will be used in the present paper, while annealing temperature extrapolation and crystallization kinetics lead to values of 523 K and 518 K, respectively [2]. The heat of fusion for a 100% crystalline sample, as estimated by diluent measurements, is reported as 14.85 kJ/mol [2].

In this paper, heat capacities are reported from 140 K to 540 K. These experimental data are analyzed using the Advanced THERMAL Analysis System, ATHAS, by computing the heat capacities of the solid from an approximate vibrational spectrum fitted to the limited experimental data. The liquid heat capacities are compared with those derived using an empirical addition scheme. Using these data for the limiting states, it was possible fully to analyze the thermodynamics of this polymer and determine the enthalpy, entropy, and Gibbs function. In addition, the solid and the liquid heat capacities enable us to

determine the change in heat capacity ( $\Delta C_p$ ) at the glass transition temperature ( $T_g$ ). For the semicrystalline PPVL in the region above the glass transition temperature, the occurrence of a "rigid amorphous" fraction is likely. This will be discussed together with the analysis of the broad melting region that can now be separated from the increase in heat capacity with temperature using the calculated baselines of solid and liquid heat capacities. Rigid amorphous fractions have previously been observed in a large number of polymers analyzed in our laboratory. These include: poly(oxyethylene), POM [4, 5]; poly(ethylene terephthalate), PET [6]; poly(oxy-1,4-phenylene-oxy-1,4-phenylene-carbonyl-1,4-phenylene), PEEK [7]; poly(thio-1,4-phenylene), PPS [8]; poly(butylene terephthalate), PBT [9]; poly(ethylene-2,6-naphthalene-dicarboxylate), PEN [10]; and poly(oxy-2,6-dimethyl-1,4-phenylene), PPO [11]. In case of PBT, the rigid amorphous fraction leads to a second glass transition about 60 K higher than the first one, while in most other polymers the rigid amorphous fraction remains metastable up to the melting temperature. In polypropylene a decreasing rigid amorphous fraction reaching zero at the beginning of melting was reported [12]. For poly(thio-1,4-phenylene), in addition to the thermal analysis [8] of the rigid amorphous fraction dielectric relaxation spectroscopy was used to demonstrate the existence of rigid amorphous fraction above the glass transition temperature [13].

The rigid fraction in a polymer can be determined from the following relationship:

$$f_r = 1 - (\Delta C_p^e / \Delta C_p^a), \quad (1)$$

where  $\Delta C_p^e$  and  $\Delta C_p^a$  represent the heat capacity increase at  $T_g$  above that of the fully rigid polymer (crystal or glass) for the semicrystalline samples (e) and the liquid PPVL (a), respectively.

The crystallinity ( $w^c$ ) of the sample is determined from the heat of fusion using the relationship:

$$w^c = \Delta H_f^e / \Delta H_f^a, \quad (2)$$

where  $\Delta H_f^a$  is the heat of fusion for the 100% crystalline sample, reported as 14.85 kJ/mol [2], and  $\Delta H_f^e$  is the experimental heat of fusion of the semicrystalline polymer. In cases where the two-phase crystallinity model is valid,  $f_r$  should be equal to  $w^c$ . If a rigid amorphous fraction exists above the glass transition region then  $f_r$  is more than  $w^c$ .

## Computations

At ATHAS, our laboratory for Advanced Thermal Analysis System, the analysis of heat capacities of more than 100 solid polymers based on approximate vibrational spectra has been completed [14–30]. This included the series of nine aliphatic polyesters [25]. The discrepancy between the experimental and computed heat capacity is less than  $\pm 3\%$  in most cases. Therefore, it was considered worthwhile to extend

this knowledge to the poly(pivalolactone) and gain more information on its thermal properties. The details of the computation have previously been described in detail [31–33]. In principle, heat capacity at only one temperature is needed to estimate the heat capacity of the solid from about 100 K to melting. To cover the whole temperature range from 0 K to melting, a second data point in the temperature range from 20 K to 50 K is needed. For the computations the vibrational spectrum is arbitrarily separated into group and skeletal vibrations. The strongly coupled skeletal vibrations are usually well approximated by the Tarasov equation, in which the parameters  $\Theta_3$  and  $\Theta_1$  represent the intermolecular and the intramolecular frequencies ( $\Theta = h\nu/k$ , where  $\nu$  is the frequency in Hz and  $h$  and  $k$  are Planck's and Boltzmann's constants, respectively;  $\Theta$  is expressed in kelvin ( $1 \text{ cm}^{-1} = 1.4388 \text{ K}$ )). These two parameters are obtained by fitting the limited experimental heat capacities below the glass transition temperature to the Tarasov equation, which is represented as follows:

$$\begin{aligned} C_v/NR &= T(\Theta_1/T, \Theta_3/T) \\ &= D_1(\Theta_1/T) - (\Theta_3/\Theta_1) \\ &\quad \times [D_1(\Theta_3/T) - D_3(\Theta_3/T)], \end{aligned} \quad (3)$$

where  $D_1$  and  $D_3$  represent the one- and three-dimensional Debye functions. Detailed discussions of the functions and computer programs for evaluation are given in references [31].

The group frequencies are coupled only to a limited degree. These are retrieved from IR and Raman data and their normal mode distribution can be approximated by Einstein functions  $E$  (single frequencies) and box distributions  $B$  (wider range frequencies), which can be represented as:

$$C_v/NR = E(\Theta_E/T) = \frac{(\Theta_E/T)^2 \exp(\Theta_E/T)}{[\exp(\Theta_E/T) - 1]^2}, \quad (4)$$

$$\begin{aligned} C_v/NR &= B(\Theta_U/T, \Theta_L/T) \\ &= \frac{\Theta_U}{\Theta_U - \Theta_L} [D_1(\Theta_U/T) - (\Theta_L/\Theta_U)D_1(\Theta_L/T)]. \end{aligned} \quad (5)$$

Computer programs of the fitting routines and computations of equations (4) and (5) are given in reference [32]. Having thus established the vibrational spectrum, it is inverted to  $C_v$ . The  $C_p$  to  $C_v$  conversion is made using the empirical Nernst-Lindemann equation [34, 35]:

$$C_p - C_v = 3RA_0(\text{new})C_p^2T/(C_v T_m^2). \quad (6)$$

Based on experimental expansivity ( $\alpha$ ) and compressibility ( $\beta$ ) for a large number of polymers, a universal value of  $3.9 \times 10^{-3} \text{ (K mol/J)}$  was obtained for the  $A_0(\text{new})$  in the ATHAS data bank for cases where  $\alpha$  and  $\beta$  are not known, as for PPVL.

## EXPERIMENTAL

### Samples

The sample of poly(pivalolactone) was obtained from Polysciences. The molecular mass was 250 000. It was a white powder, and was used as such for transition and heat capacity measurements.

### Instruments and Experiments

Phase transition measurements were performed both with a Perkin–Elmer DSC-7 and a TA Instruments DSC. Mechanical refrigeration was used in case of DSC-7, while liquid nitrogen was used for the TA Instruments DSC to cool to 210 K and 140 K, respectively. Both the temperature and heat of fusion were calibrated using standard materials (tin (505.05 K), indium (429.5 K), naphthalene (353.42 K), and *n*-dodecane (263.5 K)) in the case of DSC-7. Areas were determined using the software supplied by Perkin–Elmer. The temperature calibration in case of TA Instruments DSC was carried out using cyclohexane (186.1 K, 279.7 K), cycloheptane (134.75 K, 265.13 K), 1-chlorobutane (150.05 K), naphthalene (353.42 K), tin (505.05 K), and indium (429.75 K). Typical sample masses used in both cases were 15–20 mg, and all measurements were carried out with a heating rate of 10 K/min and a nitrogen flow rate of about 20 ml/min.

Heat capacity measurements from 150 K were carried out on a TA Instruments 2100 thermal analyzer, modified specially to carry out the low-temperature measurement [36]. The temperature calibration was carried out using the standards described above. In addition, the heat capacity data were corrected for temperature lag, asymmetry of the three measuring positions, and heating rate using the computer program developed in our laboratory [37]. Details of the techniques are described in reference [36]. Heat capacity measurements of sapphire ( $\text{Al}_2\text{O}_3$ ) were reproducible to  $\pm 0.1\%$  on the basis of data from the National Bureau of Standards (NIST) [38]. The heat capacities of the polymer were determined in three different temperature ranges: range I was from 140 K to 370 K, range II from 310 K up to 540 K, and range III from 510 K to 550 K.

Thermal stability of the samples was investigated using thermogravimetry. Nitrogen was used as a purge gas. The heating rate was 10 K/min.

## RESULTS

### Thermogravimetry

The results of thermogravimetry for PPVL showed it to be stable up to about 560 K (temperature of 0.1% mass loss). Hence the heat capacity measurements were limited to slightly below 550 K, so that there was no effect of the change in mass of the sample.

### DSC of the Transitions

The transitions for the as-received sample were investigated from 310 to 540 K using a TA Instruments DSC: the trace is shown in Fig. 1. Two

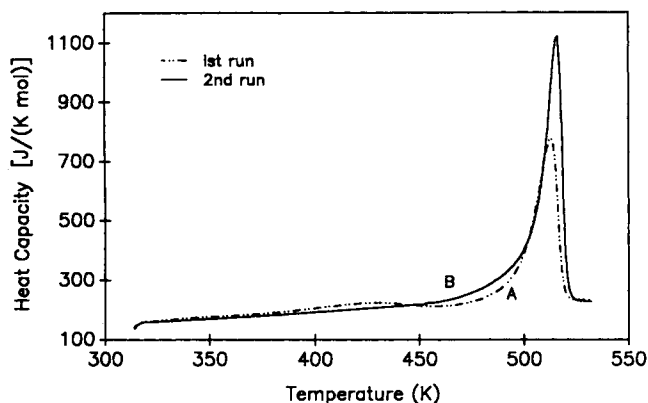


**FIGURE 1.** Heat capacity of poly(pivalolactone) measured at 10 K/min. Curve A is for as-received sample and curve B is for the sample air-cooled from the melt.

distinct transitions were observed on the initial run (A). The first transition had its onset at about 380 K and a shallow peak at 421.5 K. The high-temperature transition had an onset at 497 K and a peak temperature at about 511 K. The respective heats of transition had an onset at 497 K and a peak temperature at about 511 K. Reheating the sample cooled at an uncontrolled rate in air from 540 K showed only the higher-temperature transition, with a broad beginning (B). The onset and the peak temperature were 502 K and 513.3 K, respectively, and the heat of the transition was 10.06 kJ/mol. This peak temperature agreed with that reported in the literature [2]. The estimated crystallinity of the as-received sample, estimated from the combined heats of transition from the first run, is about 51%. For this calculation the heat of fusion for 100% crystalline sample was taken as 14.85 kJ/mol and was obtained from reference [2]. The crystallinity increased to about 68% for the air cooled sample. An as-received sample cooled to 140 K before measurement showed, in addition to the high-temperature transitions, a possible small glass transition in the temperature range 260–280 K. As will be described later, this was detected much more clearly in the heat capacity measurements.

An attempt was made to quench the sample. For this, a sample was heated to 540 K, held for about 3 min and then quenched in liquid nitrogen. It was then loaded into the calorimeter at 140 K and heated to 370 K. Melting peaks arising from melting of the unavoidable ice complicated the observation of the glass transition somewhat. An estimate of the glass transition showed a value of 259.8 K for half devitrification. A glass transition was reported at 263 K for ultraquenched PPVL samples, in good accord with our value [39]. The corresponding change in heat capacity was estimated using the baselines of the recording and found to be about 44 J/(K mol), in good accord with the computed value of 38 J/(K mol) discussed below. Furthermore, we tried to cool PPVL from the melt at the fastest possible cooling in the calorimeter, but the quenching within the instrument was not effective. The samples remained highly crystalline and showed no obvious glass transition.

### Heat Capacities measured by DSC

**Solid State Below the Glass Transition** Heat capacities were measured for PPVL covering the entire region from 150 K up to 540 K, quantitatively to analyze the nature of the observed transitions. For the solid from 140 to 260 K, the data were collected and averaged from five measurements, which agreed with one another with an RMS of  $\pm 1\%$ . Discarding the first few data points, the smoothed heat capacities from 150 K to 260 K can be described by the equation:

$$C_p = \exp[-48.06197 + 27.29137(\ln T) - 4.791726(\ln T)^2 + 0.28686(\ln T)^3](\pm 0.3\%). \quad (7)$$

### Semicrystalline State Above the Glass Transition

The heat capacities through the glass transition and above the glass transition region (estimated to be in the range of 260–280 K) are shown in Table 1. From 270 to 530 K the heat capacities were smoothed by spline function interpolation. Data for two additional thermal histories (columns 3 and 4) are also shown in Table 1.

**Melt Region** For the heat capacities of the melt an average of 15 measurements on samples of different size masses was computed. Measurements could be made from 510 K to 550 K, resulting in the following smoothed equation:

$$C_p = 112.4 + 0.221T \quad (\pm 0.13\%) \text{ in } [J/(K \text{ mol})]. \quad (8)$$

### Computation of the Heat Capacity of the Solid

The experimental heat capacity from 150 K to 360 K was fitted to an approximate vibrational spectrum using the *ATHAS* computation scheme described earlier in the text. The vibrational spectrum was separated into 14 skeletal modes and 31 group vibrational modes. The chosen frequencies are listed in Table 2. The group vibrations for the  $-\text{COO}$  group were obtained from reference [25] and found earlier also to work well in the case of the series of linear polyesters. For  $-\text{CH}_2$  and the  $-\text{C}(\text{CH}_3)_2$ , the frequencies were retrieved from the normal-mode calculations of polyethylene [28] and that of polyisobutylene [22]. Subtracting the group vibrational contribution from the heat capacity at constant volume ( $C_v$ ), the skeletal heat capacity was inverted by the Tarasov equation, equation (3), to give  $\Theta_1$  temperatures. From 150 K to 260 K the value of  $\Theta_1$  remained approximately constant, at an average of  $564.9 \text{ K} \pm 16.6 \text{ K}$ . Beyond 260 K,  $\Theta_1$  showed a gradual decrease to 278 K at 360 K. This decrease in  $\Theta_1$  agrees with the occurrence of a broad glass transition. Since no heat capacities were measured below 150 K,  $\Theta_3$  could not be evaluated and a value of 98 K was estimated to represent the intermolecular contribution to the skeletal heat capacity. This estimate is

based on low-temperature heat capacities of polyglycolide analyzed earlier in our laboratory, and on the knowledge that similar polymers have similar values of  $\Theta_3$  [25]. The  $C_p$  to  $C_v$  conversion was made using the universal  $A_0$  value of  $0.0039 \text{ (K mol)/J}$ . The heat capacities were then computed from 0.1 to 1000 K using the above-described  $\Theta_1$  and  $\Theta_3$  temperatures and the various group vibrations of Table 2. The average and the RMS error of the calculated heat capacity from that of the experimental data was  $-0.02 \pm 1.0\%$  from 150 to 270 K. The deviation of the calculated data from the experiment is shown in Fig. 3. From 150 K to about 240 K, calculated and experimental data agreed, with errors of less than 1%. Above 260 K the experimental heat capacities were increasingly higher than the calculated  $C_p$  and at 370 K the error was as high as 5% and most likely caused by the glass transition.

**TABLE 1.** Heat Capacity of Poly(pivalolactone).

Temperature (K)	Heat capacity (J/(K mol))		
	(a)	(b)	(c)
260	128.3	n.a.	126.0
270	136.5	n.a.	132.6
280	142.4	n.a.	138.2
290	146.9	n.a.	143.5
300	151.0	n.a.	148.2
310	154.9	n.a.	153.3
320	159.9	158.6	157.8
330	165.0	162.4	162.7
340	170.0	166.2	167.1
350	174.4	169.8	171.6
360	179.0	173.6	175.6
370	184.3	178.2	179.1
380	191.0	182.6	181.8
390	197.8	187.7	183.3
400	206.0	192.4	183.0
410	213.5	197.2	181.8
420	220.8	202.4	180.7
430	223.8	207.8	182.4
440	219.7	212.5	189.1
450	213.3	219.0	201.3
460	212.2	228.0	217.3
470	219.3	244.1	238.1
480	237.6	272.0	264.6
490	278.0	316.6	318.3
500	389.1	402.6	512.5
505	522.3	502.0	1065.6
510	713.8	723.2	999.1
515	691.6	1110.7	354.0
520	256.4	379.4	252.5
530	233.2	227.9	225.8

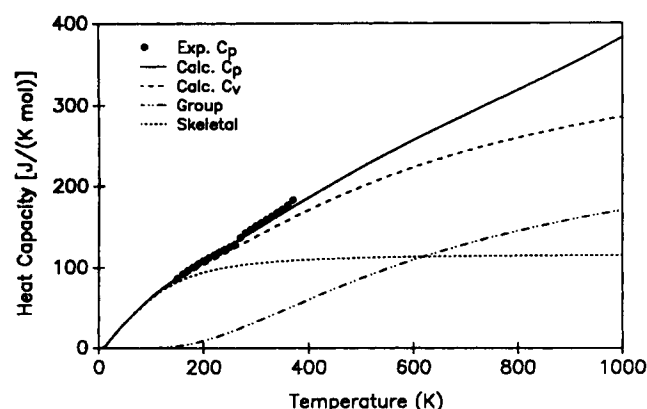
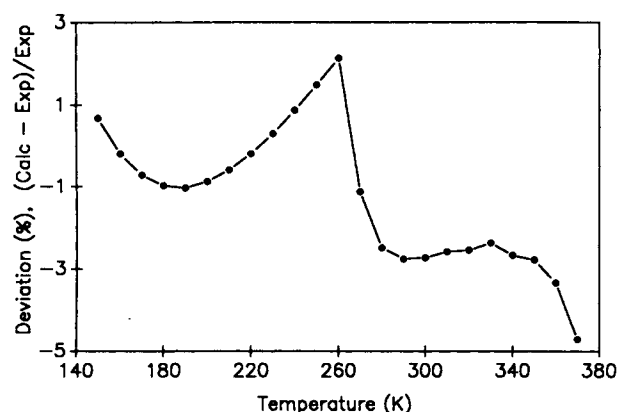
(a) From 150 to 260 K the data are described as given in the text by equation (5). The data from 270 to 530 K were smoothed by a spline function. Measurements from 270 to 310 K refer to a sample cooled from room temperature to 140 K and then heated at 10 K/min. From 320 to 530 K, the data were measured for the as-received sample and averaged from 320 to 370 K with those for the sample cooled to 140 K. From 510 to 550 K, the heat capacities of the melt are described by equation (6).

(b) Data from 310 to 540 K for a sample cooled in air from 540 to 310 K.

(c) Data for a sample cooled at 320 K/min from the melt using the DSC 7.

**TABLE 2.** Group Vibration Frequencies in Kelvin ( $h\nu/k$ )

Approximate vibrational mode	N	Frequency (K)
(a) $-\text{CH}_2^a$		
CH <sub>2</sub> asym. stretch	1	4181.1
CH <sub>2</sub> sym. stretch	1	4097.7
CH <sub>2</sub> bend	1	2074.7
CH <sub>2</sub> wag	0.35	1976.6
	0.65	1698.3–1976.6
CH <sub>2</sub> twist	0.52	1874.3
	0.48	1689.6–1874.3
CH <sub>2</sub> rock	0.04	1494.1
	0.59	1038.0–1494.1
	0.37	1079.1
(b) $-\text{C}(\text{CH}_3)_2^b$		
CH <sub>3</sub> asym. stretch	2	4262.0
CH <sub>3</sub> asym. stretch	2	4259.0
CH <sub>3</sub> sym. stretch	2	4147.0
CH <sub>3</sub> asym. bend	2	2107.0
CH <sub>3</sub> asym. bend	2	2101.0
CH <sub>3</sub> sym. bend	0.5	1987.0
	0.76	1973.0–1983.0
	0.74	1973.0
CH <sub>3</sub> stretch and rock	6.0	1164.0–1680.0
(c) $-\text{COO}^c$		
C=O stretch	1	2530.0
C–O stretch	1	1800.0
O–C stretch	0.22	1385.1
	0.11	1632.1
	0.67	1385.1–1632.1
C=O in-plane bend	1	980.0
C=O out-of-plane bend	1	840.0
(d) CH <sub>2</sub> –COO chain stretch <sup>c</sup>		
CH <sub>2</sub> –COO stretch	1	1215.0
(e) C–C stretch (backbone) <sup>b</sup>		
C–C stretch	0.17	1197.0
	0.28	1167.0
	0.55	1167.0–1198.0

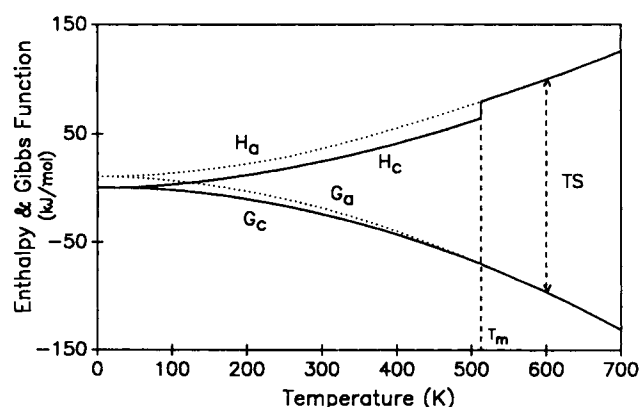
<sup>a</sup> From normal mode calculations of polyethylene [22].<sup>b</sup> From the frequencies used for poly(isobutylene) [22].<sup>c</sup> From the frequencies used for linear polyesters [25].**FIGURE 2.** Heat capacity computed from the approximate vibrational spectrum, consisting of 14 skeletal and 31 group vibrational modes.**FIGURE 3.** Deviation of the experimental heat capacity obtained from equation (7) in the text, from the calculated data.

### Thermodynamic Functions

Thermodynamic functions (enthalpy, entropy, and Gibbs free energy) can be derived from the heat capacity by integration. A plot of the enthalpy, Gibbs function, and TS for the crystalline state and for the amorphous state is shown in Fig. 4. Detailed tables of these functions are contained in the *ATHAS* Data Bank and can be obtained on request from the second authors [14]. In the case of PPVL, since information on the equilibrium heat of fusion and the melting temperature was available in the literature, and a glass transition temperature could be obtained at 260 K through the new heat capacity measurements, one could also calculate the residual entropy of glass at absolute zero:

$$S_0^a = \int (C_p^c - C_p^a) d(\ln T) + \Delta S_f^o, \quad (9)$$

where  $\Delta S_f^o$  is the entropy of fusion ( $\Delta S_f^o = \Delta H_f^o / T_m^o$ ),  $C_p^c$  and  $C_p^a$  are the crystalline and amorphous heat capacities, respectively. In deriving the thermodynamic functions, the *ATHAS* computed heat capacities for the solid and the smoothed experimental liquid

**FIGURE 4.** Thermodynamic functions of crystalline and amorphous poly(pivalolactone).

data were used. Below the glass transition temperature both the crystalline and the glassy heat capacities were assumed to be the same, as no heat capacities were available for the data below 50 K. Although it is well known that amorphous  $C_p$  is higher below 50 K, its contribution to the integral function is too small to cause significant differences in the derived functions. The residual entropy for the amorphous state at 0 K was obtained at 15.5 J/(K mol). Since the chemical structure of PPVL( $\text{CH}_2$ —)[ $\text{C}(\text{CH}_3)_2$ —](COO—) corresponds to three mobile beads in the backbone repeat unit, the residual entropy at 0 K (and  $T_g$ ) relative to the crystalline PPVL is 5.16 J/(K mol).

## DISCUSSION

### Heat Capacities in the Solid State

Using the experimental heat capacities below the glass transition temperature, it was possible to calculate the "vibration-only"  $C_p$ , as had been done earlier for more than 100 polymers available in the ATHAS data bank [14]. Separating the frequency spectrum into 14 skeletal modes and 31 group vibrational modes is a reasonable choice, justified by the agreement between calculated and experimental heat capacities within the experimental uncertainty of  $\pm 3\%$ . It was suggested for polyisobutylene (PIBUT) that the limit of usefulness of the Tarasov equation had been reached, as the deviations between the calculated  $C_p$  and experimental  $C_p$  at low temperatures were beyond the experimental uncertainty ( $\sim 30\%$  at 15 K and  $\sim 10\%$  at 80 K). In the case of PPVL the lowest available data were at 150 K, and it was not possible to analyze the  $C_p$  calculated at low temperature. In the narrow range of experimental data from 150 K up to 260 K in PPVL and from above 80 K to 200 K ( $T_g$ ), it appears that in this range the Tarasov equation can be used to represent the skeletal modes in the vibrational spectrum, as the agreement between the calculated and the experimental heat capacities was better than 1%.

PPVL has an additional  $-\text{C}(\text{CH}_3)_2$  group when compared to the repeating unit of polyglycolide (PGL) [25], and the presence of this increases the  $\Theta_1$  temperature from 521 K for PGL to 565 K for PPVL. However, this value is much lower than  $\Theta_1$  for PIBUT [22], for which the  $\Theta_1$  temperature was 850 K, which indicated a relatively stiffer backbone. These results thus indicate that, for PPVL, the presence of the ester linkage in the backbone makes the backbone more flexible than PIBUT, and this is reflected in the lowering of the  $\Theta_1$  temperature, which is a measure of the intramolecular contributions to the heat capacity.

### Heat Capacities in the Liquid State

The heat capacity for liquid PPVL exhibited a linear temperature dependence, as had been observed for a large number of liquid polymers in the ATHAS data bank. The reason for such a linear increase is quantitatively not well understood. An attempt was made

in our laboratory [40] to approximate the vibrational, conformational, and external parts of the partition function of the liquid polyethylene on the basis of its detailed PVT data and statistical thermodynamics. In this attempt, the linear heat capacities resulted from an approximate cancellation of the nonlinearity of the three contributions. The extension of this treatment to other linear macromolecules is hindered due to the lack of PVT information. At present, the large volume of the data on the liquid state of the polymers in our data is correlated only by empirical equations [41–43].

In the data bank, tables of heat capacity contributions are available for the molten state of various groups present in the repeating unit of poly(pivalolactone). For the  $-\text{CH}_2$  and  $-\text{C}(\text{CH}_3)_2$  groups, the melt heat capacities were obtained from the smoothed experimental heat capacities of polyethylene [44] and polyisobutylene [45]. The data for the  $-\text{COO}$  group were obtained from the equation describing the molten data for eight polylactones and poly(ethylene sebacate) [46]. The heat capacities for the various groups were empirically added and the data compared to the experimentally obtained liquid data for PPVL, as is presented by equation (8). The average and RMS error of the addition scheme data from the experimental data from 240 K to 550 K was  $-4.9\% \pm 2.8\%$ , while from 510 K to 550 K the average and RMS error was  $-8.7\% \pm 0.3\%$ . For the COO group and the  $\text{C}(\text{CH}_3)_2$  group the melt heat capacities were present only up to 400 K, and beyond this the data was extrapolated. The higher errors at temperatures beyond 400 K cast doubt on the usefulness of the extrapolated melt heat capacities.

### Glass Transition Region

Semicrystalline PPVL showed a small but distinct glass transition temperature at 267.3 K, detected only through the heat capacity measurements and its analysis in terms of the approximate vibrational spectrum. Using the calculated solid heat capacities and the smoothed liquid experimental  $C_p$ , it was possible to estimate the glass transition temperature by comparing the experimental heat capacities in the region from 190 K to 340 K. In Fig. 5 the plot of the experimental data is shown together with the calculated  $C_p$  for the as-received, air-cooled and fast-cooled samples (320 K/min). The  $\Delta C_p^s$  at a  $T_g$  of 267.3 K for the semicrystalline as-received sample is 7.9 J/(K mol). From the values of the heat capacity of the limiting states (calculated solid and smoothed liquid) at the glass transition temperature, the  $\Delta C_p^a$  for the 100% amorphous PPVL is calculated to be 38.8 J/(K mol). Using this value in the relationship  $\alpha = (1 - \Delta C_p^s / \Delta C_p^a)$ , the crystallinity,  $\alpha$ , was calculated to be 78.9% for the semicrystalline polymer. As will be seen in the next section, the crystallinity obtained from the heat of fusion was lower, and this indicated the probable existence of some rigid amorphous fraction in PPVL.

The estimate of the  $T_g$  value in the quenched samples analyzed through transition measurements showed it to occur at 259.8 K, which was lower than

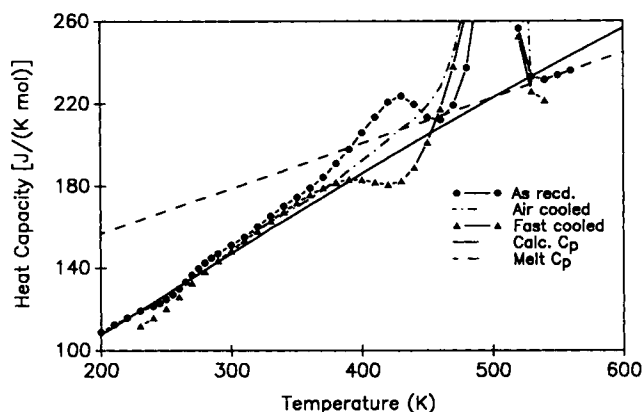


**FIGURE 5.** Experimental heat capacities of the samples prepared at different thermal histories and compared with the calculated  $C_p$  data and the linearly extrapolated melt data.

that for the semicrystalline samples (267.3 K). Such an increase in  $T_g$  on partial crystallization is frequently observed in linear macromolecules. The approximate experimental value of  $\Delta C_p$  for amorphous PPVL was 44 J/(K mol) and is sufficiently close to the  $\Delta C_p^a$  of 38.8 J/(K mol) for 100% amorphous PPVL. This value of  $\Delta C_p^a$  can be analyzed from the standard interpretation of the change in heat capacity at the glass transition temperature. The contribution to  $\Delta C_p$  of a small bead has been well established at 11.5 J/(K mol) [47] and has been found to be size dependent. The bulky groups referred to as large beads usually contribute double the value for a small bead. The series of polylactones from polyglycolide to polycaprolactone [46] showed a higher  $\Delta C_p$  at  $T_g$  than that expected for small beads, while polyisobutylene [14] had a value of only 21.3 J/(K mol), corresponding to small beads. Although the assignment of the groups in terms of beads is not precise one can, from the analysis of polylactones and polyisobutylene, estimate that three beads gain mobility at the glass transition temperature in the case of PPVL, and 34.5 J/(K mol) is in reasonable agreement with the computed  $\Delta C_p$  of 38.8 J/(K mol).

#### Rigid Amorphous Fraction above the Glass Transition Temperature

Having established the solid (calculated) and liquid (smoothed experimental) heat capacities as the base-lines, it was possible to determine the rigid fraction in the region above the glass transition temperature and its change up to the melting transition. In Table 3 are shown the rigid fraction and the rigid amorphous fraction calculated using equations (1) and (2) for the as-received sample (A) and the one crystallized by cooling in air from that of the melt (B) (see also Fig. 1). Both samples contained a rigid fraction in the semicrystalline region above the glass transition temperature. Sample A had an average rigid amorphous fraction of about 0.37, estimated in the temperature range from 290 K to 310 K. Sample B

showed a smaller "rigid amorphous" fraction of 0.19, estimated from 310 K to 360 K. The increase of the rigid amorphous fraction with the cooling rate is also common in the other examples analyzed [7–11]. The change of the rigid amorphous fraction with temperature merges with the beginning of fusion of the  $\gamma$  form in sample A (beginning at about 330 K) and the  $\alpha$  form of sample B (beginning at about 370 K). Because of the higher portion of a constant rigid amorphous fraction for sample B it is likely that the rigid amorphous fraction is only lost with the melting range of the  $\alpha$ -crystals and much, if not all, of the heat capacity increase of sample A from 330 to 400 K is due to the  $\gamma$ - $\alpha$  transition, and not to the glass transition of the rigid amorphous fraction. To verify this assumption, the heat capacity of the as-received sample was also measured from room temperature up to only 460 K (above the  $\gamma$ - $\alpha$  transition, but before melting) and compared to the heat capacity of the same samples cooled in air from 460 K and reheated at 10 K/min. The second heating led to a somewhat lower heat capacity ( $\sim 4\%$  at 350 K and  $\sim 8\%$  at 390 K), indicating that some, but not all, of the rigid amorphous fraction is lost on annealing at 460 K. Similarly, the increase in heat capacity observed in this annealed sample may also be partially or fully due to early melting of small crystals [3].

In the polylactones analyzed earlier [46], due to the unavailability of an estimate for the heat of fusion for 100% crystallinity, an analysis of the rigid amorphous fraction was not possible. In these polymers the crystallinity evaluated from the  $\Delta C_p$  at the glass transition temperature was used to estimate the heat of fusion. These estimates of heat of fusion would be too low if a rigid amorphous fraction was also present in these polymers. An indication that the straight-chain, aliphatic polyesters may not have a rigid amorphous fraction is given by the analysis of poly(ethylene sebacate) (PES). Its heat capacity for a semicrystalline sample with known crystallinity (52%) was reported [48] to be above the glass transition temperature (245 K). The heat capacities of the semicrystalline sample from 250 to 320 K computed

**TABLE 3.** Rigid Fraction in Semicrystalline PPVL<sup>a</sup>

Temperature (K)	Total rigid fraction		Rigid amorphous fraction	
	A	B	A	B
290	0.88	n.a.	0.38	n.a.
300	0.87	n.a.	0.37	n.a.
310	0.87	0.87	0.37	0.19
320	0.82	0.87	0.32	0.19
330	0.78	0.88	0.28	0.20
340	0.71	0.86	0.21	0.18
350	0.66	0.86	0.16	0.18
360	0.61	0.86	0.11	0.18
370	0.51	0.81	0.00	0.13

<sup>a</sup> A is the as-received sample of crystallinity 0.5, and B is the sample crystallized by cooling in air of crystallinity 0.68.

from the known crystalline  $C_p$  and the liquid  $C_p$  (ATHAS Data Bank values) showed no evidence of a rigid amorphous fraction. Rather, the computed heat capacity was somewhat lower than the experimental data, suggesting higher heat capacities due to a broad premelting region reaching from the melting peak temperature (245 K) to the glass transition. At present, the existence of a rigid amorphous fraction in aliphatic polyesters can only be shown with certainty in the case of poly(pivalolactone).

### Thermodynamic Functions

The residual entropy obtained for the amorphous state at 0 K was 15.5 J/(K mol). If one considers, as suggested in the glass transition discussion, three mobile units in the repeating unit of the polymer, then each bead contributes about 5.16 J/(K mol) to the residual entropy. This value compares well with the average value of 5.3 J/(K mol) for the linear polyesters of eight polylactones and poly(ethylene sebacate). This value is higher than most of those analyzed in the ATHAS Data Bank. Higher values of  $S_0^\circ$  were also observed for the aliphatic polyamides [49], in which each mobile bead was reported to contribute about 5–7 J/(K mol).

### ACKNOWLEDGMENTS

This work was supported by the Division of Materials Research, National Science Foundation, Polymers Program, Grant #DMR 8818412 and the Division of Materials Sciences, Office of Basic Energy Sciences, U.S. Department of Energy, under Contract DE-AC05-84OR21400 with Martin Marietta Energy Systems, Inc.

### REFERENCES

1. R. E. Prud'homme and R. H. Marchessault, *Makromol. Chem.*, **175**, 2705 (1974).
2. C. Borri, S. Brückner, V. Crescenti, G. Fortuna Della, A. Mariano, and P. Scarazzato, *Eur. Polym. J.*, **7**, 1515 (1971).
3. B. Wunderlich, Crystal melting, in *Macromolecular Physics*, Vol. 3, Academic Press (1980), p. 184.
4. H. Suzuki and B. Wunderlich, *J. Polym. Sci., Polym. Phys. Ed.*, **23**, 1671 (1985).
5. H. Suzuki, J. Grebowicz, and B. Wunderlich, *Makromol. Chem.*, **189**, 1109 (1985).
6. J. Menczel and B. Wunderlich, *J. Polym. Sci., Polym. Letters Ed.*, **19**, 261 (1981).
7. S. Z. D. Cheng, M. Y. Cao, and B. Wunderlich, *Macromol.*, **19**, 1868 (1986).
8. S. Z. D. Cheng, Z. Q. Wu, and B. Wunderlich, *Macromol.*, **20**, 2802 (1987).
9. S. Z. D. Cheng, R. Pan, and B. Wunderlich, *Makromol. Chem.*, **189**, 2443 (1988).
10. S. Z. D. Cheng and B. Wunderlich, *Macromol.*, **21**, 789 (1988).
11. S. Z. D. Cheng and B. Wunderlich, *Macromol.*, **20**, 1630 (1987).
12. J. Grebowicz, S.-F. Lau, and B. Wunderlich, *J. Polym. Sci., Polym., Symp.*, **71**, 19 (1984).
13. P. Huo and P. Cebe, *Mat. Res. Soc. Symp. Proc.*, **215**, 93 (1991).
14. ATHAS Data Bank, Department of Chemistry, University of Tennessee, Knoxville, TN 37996-1600, U.S.A.
15. M. Varma-Nair, Y. Jin, and B. Wunderlich [polysulfones], *Polymer*, to be published (1992).
16. M. Varma-Nair, J. Cheng, Y. Jin, and B. Wunderlich [poly(silylenes)], *Macromolecules*, **24**, 5442 (1991).
17. Y. Jin and B. Wunderlich [paraffins], *J. Phys. Chem.*, **95**, 9000 (1991).
18. K. Roles and B. Wunderlich [poly(amino acids)], *Biopolymers*, **31**, 477 (1991).
19. A. Xenopoulos and B. Wunderlich [polyamides], *Polymer*, **31**, 1260 (1990).
20. S. Z. D. Cheng, R. Pan, and B. Wunderlich [poly(butylene terephthalate)], *Makromol. Chem.*, **189**, 2443 (1988).
21. H. S. Bu, W. Aycock, S. Z. D. Cheng, and B. Wunderlich [14 various polymers], *Polymer*, **29**, 1485 (1988).
22. H. S. Bu, W. Aycock, and B. Wunderlich [various branched polymers], *Polymer*, **28**, 1165 (1987).
23. S. Z. D. Cheng, S. Lim, L. H. Judovits, and B. Wunderlich [high melting phenylene containing polymers], *Polymer*, **28**, 10 (1987).
24. L. Judovits, R. C. Bopp, U. Gaur, and B. Wunderlich [polystyrenes], *J. Polym. Sci., Polym. Phys. Ed.*, **24**, 2725 (1986).
25. S. Lim and B. Wunderlich [aliphatic polyesters], *Polymer*, **28**, 777 (1987).
26. M. Loufakis and B. Wunderlich [chlorine and fluorine containing derivatives of polyethylene], *Polymer*, **27**, 563 (1986); **26**, 1875 (1985).
27. J. Grebowicz, W. Aycock, and B. Wunderlich [1,4-polybutadienes], *Polymer*, **27**, 575 (1986).
28. J. Grebowicz, H. Suzuki, and B. Wunderlich [polyethylene and aliphatic polyoxides], *Polymer*, **26**, 561 (1985).
29. S. F. Lau, H. Suzuki, and B. Wunderlich [polytetrafluoroethylene] *J. Polym. Sci., Polym. Phys. Ed.*, **22**, 379 (1984).
30. J. Grebowicz, S. F. Lau, and B. Wunderlich [polypropylene], *J. Polym. Sci., Symposia*, **71**, 19 (1984).
31. Y. Cheban, S. F. Lau, and B. Wunderlich, *Colloid Polym. Sci.*, **260**, 9 (1982).
32. S. F. Lau and B. Wunderlich, *J. Thermal Anal.*, **28**, 59 (1983).
33. R. Pan, M. Varma-Nair, and B. Wunderlich, *J. Thermal Anal.*, **36**, 145 (1990).
34. J. Grebowicz and B. Wunderlich, *J. Thermal Anal.*, **30**, 229 (1985).
35. R. Pan, M. Varma-Nair, and B. Wunderlich, *J. Thermal Anal.*, **35**, 955 (1989).
36. Y. Jin and B. Wunderlich, *J. Thermal Anal.*, **36**, 765 (1990); **36**, 1519 (1990).
37. Y. Jin and B. Wunderlich, *J. Thermal Anal.*, to be published (1992).
38. D. C. Ginnings and G. T. Furukawa, *J. Am. Chem. Soc.*, **75**, 522 (1953).
39. P. H. Geil, Ultraquenching, double  $T_g$ , order and motion in amorphous polymers, in *Order in the Amorphous State of Polymers* ed., S. K. Keinath, R. L. Miller, and J. K. Rieke (Eds), Plenum, New York (1987), p. 83.
40. K. Lofakis and B. Wunderlich, *J. Phys. Chem.*, **92**, 4205 (1988).
41. H. Suzuki and B. Wunderlich, *J. Polym. Sci., Polym. Phys. Ed.*, **23**, 1671 (1985).
42. S. Z. D. Cheng and B. Wunderlich, *J. Polym. Sci., Polym. Phys. Ed.*, **24**, 1755 (1986).
43. S. Z. D. Cheng, R. Pan, H. S. Bu, and B. Wunderlich, *Makromol. Chem.*, **189**, 1579 (1988).



44. U. Gaur and B. Wunderlich, *J. Phys. Chem. Ref. Data*, 10, 119 (1981).
45. U. Gaur, M. Y. Cao, R. Pan, and B. Wunderlich, *J. Polym. Sci., Polym. Phys. Ed.*, 31, 421 (1986).
46. M. Varma-Nair, R. Pan, and B. Wunderlich, *J. Polym. Sci., Polym. Phys. Ed.*, 29, 1107 (1991).
47. B. Wunderlich, *J. Phys. Chem.*, 64, 1052 (1960).
48. B. Wunderlich and M. Dole, *J. Polym. Sci.*, 32, 125 (1958).
49. A. Xenopoulos and B. Wunderlich, *J. Polym. Sci., Polym. Phys. Ed.*, 28, 2271 (1990).